Articles

Titration of Histidine 62 in R67 Dihydrofolate Reductase Is Linked to a Tetramer ↔ Two-Dimer Equilibrium†

Robert Nichols,‡ C. David Weaver,‡ Edward Eisenstein,§ Raymond L. Blakley,∥ James Appleman,∥ Tai-Huang Huang,⊥ Fu-Yung Huang,⊥,ℱ and Elizabeth E. Howell*,‡

Department of Biochemistry, University of Tennessee, Knoxville, Tennessee 37996-0840, Center for Advanced Research in Biotechnology, Rockville, Maryland, Department of Chemistry and Biochemistry, University of Maryland, Baltimore County, Baltimore, Maryland 21228, Department of Biochemical and Clinical Pharmacology, St. Jude Children's Research Hospital, Memphis, Tennessee 38101, and Institute of Biomedical Sciences, Academia Sinica, Taipei, Taiwan, Republic of China

Received September 9, 1992; Revised Manuscript Received December 7, 1992

ABSTRACT: R67 dihydrofolate reductase (DHFR) is an R-plasmid encoded protein that confers clinical resistance to the antibacterial drug trimethoprim. To determine whether an acidic titration in kinetic pH profiles is related to titration of histidines 62, 162, 262, and 362, the stability of tetrameric R67 DHFR has been monitored as a function of pH. For the pH range 5–8, tetrameric R67 DHFR reversibly dissociates into dimers, as monitored by ultracentrifugation and molecular sieving techniques. From the crystal structures of dimeric and tetrameric R67 DHFR [Matthews et al. (1986) *Biochemistry 25,* 4194–4204] (Narayana, Matthews, and Xuong, personal communication), symmetry-related histidines 62, 162, 262, and 362 occur at the two dimer–dimer interfaces and protonation of these residues could destabilize tetrameric R67 DHFR. Ionization of these histidines was confirmed by monitoring the chemical shifts of the C2 proton in NMR experiments, and best fits of an incomplete titration curve yield a pK_a of 6.77. Since tryptophans 38, 138, 238, and 338 also occur at the dimer–dimer interfaces, fluorescence additionally monitors the tetramer–two dimers equilibrium. When fluorescence was monitored over the pH range 5–8, a protein concentration dependence of fluorescence was observed and global fitting of three titration curves yielded K_d = 9.72 nM and pK_a = 6.84 for the linked reactions:

$$\text{tetramer} \overset{K_d}{\leftrightarrow} 2 \text{ dimers} + 2n\ H^+ \overset{K_a^{2n}}{\leftrightarrow} 2\ n\text{-protonated dimers}$$

Modification of H62, H162, H262, and H362 by diethyl pyrocarbonate stabilizes dimeric R67 DHFR and causes a 200–600-fold decrease in catalytic efficiency. Decreased catalytic activity in dimeric R67 DHFR is presumably due to loss of the putative single active site pore found in tetrameric R67 DHFR.

Dihydrofolate reductase (DHFR[1]; EC 1.5.1.3) catalyzes the NADPH-dependent reduction of 7,8-dihydrofolate (DHF) to 5,6,7,8-tetrahydrofolate. Inhibition of chromosomally encoded DHFR results in blockage of DNA synthesis and ultimately cell death as tetrahydrofolate is required for the synthesis of thymidylate, purine nucleosides, methionine, and other metabolic intermediates (Kraut & Matthews, 1987). The active site inhibitor, trimethoprim (TMP), which selectively inhibits bacterial DHFR, has been used as a broad-spectrum antibiotic (in combination with sulfonamides).

Clinical resistance to TMP has been observed recently and is due to production of novel DHFRs encoded by R-plasmids (Amyes & Smith, 1974; Skold & Widh, 1974). At least 10 groups of R-plasmid DHFRs designated type I–type X have been identified (Pattishall et al., 1977; Fling et al., 1988; Sundstrom et al., 1987, 1988; Wylie et al., 1988; Amyes et al., 1989, 1992; Amyes, 1989; Wylie & Koornhof, 1991; Huovinen, 1987; Jansson & Skold, 1991; Parsons et al., 1991). Type II DHFR is particularly interesting as it is genetically unrelated to chromosomal DHFR. Three variants of type II DHFRs have been identified and named R67, R388, and R751 DHFRs (Flensburg & Steen, 1986; Brisson & Hohn, 1984; Swift et al., 1981).

R67 DHFR is a homotetramer (molecular weight 33 720), and each monomer consists of 78 amino acids (Smith et al., 1979). X-ray crystal structures of dimeric and tetrameric forms of R67 DHFR are available [Matthews et al. (1986); Narayana, Matthews, and Xuong, personal communication]. Surprisingly, there are no homologies to chromosomal DHFR when either the overall structure or the proposed active site is compared. Each monomer in dimeric R67 DHFR is an up and down six-stranded β-barrel with a missing fifth strand. Strands B, C, and D from one monomer associate with the

† This research was supported in part by NIH Grant GM35308 (to E.E.H.), NSF Grant DMB90-02177 (to E.E.), NIH Grant CA31922 (to R.L.B.), Cancer Core Grant P30 CA21765 (R.L.B.), and the American Lebanese Syrian Associated Charities (R.L.B.). NMR experiments were performed at the UAB NMR Core Facility which is supported by Cancer Core Grant P30 CA13148 from NIH.

‡ University of Tennessee.

§ Center for Advanced Research in Biotechnology and the University of Maryland.

∥ St. Jude Children's Research Hospital.

⊥ Academia Sinica.

ℱ Present address: Department of Chemistry, National Cheng-Kung University, Tainan, Taiwan, Republic of China.

[1] Abbreviations: DHFR, dihydrofolate reductase; TMP, trimethoprim; DHF, dihydrofolate; MTA buffer, 50 mM MES–100 mM Tris–50 mM acetic acid–10 mM β-mercaptoethanol buffer; DEPC, diethyl pyrocarbonate; T, tetramer; D, dimer; DH_n, protonated dimer with n hydrogens; pH*, uncorrected pH meter reading in ^2H_2O solutions.

0006-2960/93/0432-1695$04.00/0 © 1993 American Chemical Society

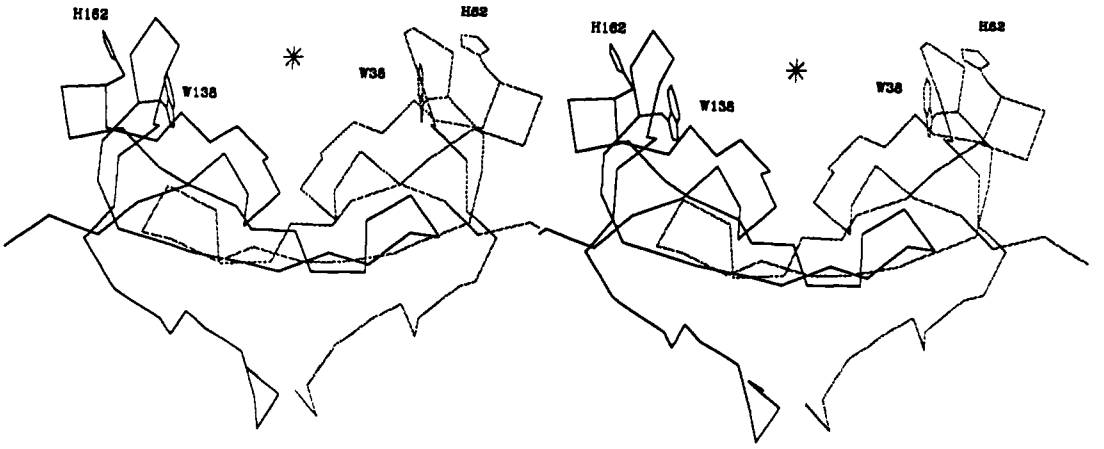

FIGURE 1: Stereo pair depicting the α-carbon backbone in dimeric R67 DHFR (Matthews et al., 1986). Monomer 1 is on the right; monomer 2 is at the left. The positions and side chains of H62 and H162 and W38 and W138 are shown. Both H62 and W38 occur in loops in the structure, not in the β-barrel core. A 222 symmetry element denoted by the central star relates the monomer of R67 DHFR to tetrameric R67 DHFR (Matthews, Xuong, and Narayana, personal communication). By performing an 180° rotation about the z axis using one of the 222 symmetry elements, H62 and W38 can be envisioned to move from an exposed, hydrophilic environment in dimeric R67 DHFR to a buried, hydrophobic environment in tetrameric R67 DHFR. The 222 symmetry operator (star) occurs at the center of the putative active site pore.

equivalent strands in the second monomer to form a third β-barrel at the monomer–monomer interface.

In the tetrameric structure, an unusual pore passes through the center of the protein (Narayana, Matthews, and Xuong, personal communication). Difference density maps describing bound thio-NADP$^+$ suggest the center of the pore is the locus for cofactor and presumably substrate binding. Of especial interest is the implication that one active site exists per tetramer and that residues from each monomer contribute to this binding site.

The catalytic efficiency [$k_{cat}/K_{m(dihydrofolate)}$] of R67 DHFR is 1% that of *Escherichia coli* chromosomal DHFR (Joyner et al., 1984; Smith & Burchall, 1983; Reece et al., 1991). Morrison and Sneddon (1990) have reported a half-bell-shaped pH profile for R67 DHFR with a single ionization (pK_a 6.4 for V/K plot, pK_a 5.8 for V plot). Brito et al. (1990) reported a bell-shaped pH profile for percent activity in their studies of RBG200 DHFR, a synthetic R388 (type II) DHFR. Their acidic pK_a value is ~5.5. These observations describing pH behavior suggest histidine residues may be ionizing in type II DHFRs and affecting enzyme activity.

A single histidine (H62) occurs per monomer in the loop connecting β-strands D and E. The crystal structure of dimeric R67 DHFR is shown in Figure 1, and the positions of H62 and H162 (second monomer)[2] are indicated (Matthews et al., 1986). Use of the crystallographic 222 symmetry operator (star in Figure 1; Matthews, Xuong, and Narayana, personal communication) on monomeric R67 DHFR generates tetrameric R67 DHFR. From Figure 1, H62 and 162 occur at the dimer–dimer interface since H62 and H162 are exposed in dimeric R67 DHFR, whereas H62 and H162 will be buried in tetrameric R67 DHFR. From the 222 symmetry operator, two histidines appear per interface. H62 and H362 occur at one dimer–dimer interface, and H162 and H262 occur at the second interface. Ionization of H62 could potentially destabilize tetrameric R67 DHFR and favor dimer formation. As the putative active site pore would be lost in dimeric R67 DHFR, decreased activity should result. In this paper, we report our preliminary investigations on the effect of protonation of H62 on tetramer stability and protein activity.

MATERIALS AND METHODS

Protein Purification. R67 DHFR was expressed and purified as previously described (Reece et al., 1991). Briefly, *E. coli* cells harboring a plasmid containing the R67 DHFR gene (P700) were grown to late stationary phase and lysed by addition of 1 M NaOH until pH 12 was reached (Vermersch et al., 1986). Cell debris was removed by centrifugation, and the lysis solution was titrated to pH 2.0. Precipitated material was removed and the solution returned to pH 7.4. After dialysis, the protein solution was applied to a 1.0 × 29 cm PBE chromatofocusing column (Pharmacia) equilibrated in 0.025 M imidazole (pH 7.4) and R67 DHFR was eluted using a 1:10 dilution of Polybuffer 74 (pH 5.0, Pharmacia). In a final purification step, the protein solution was chromatographed on a 2.5 × 88 cm G-75 Sephadex column. Protein purified by this method possesses a specific activity equivalent to protein purified using other procedures (Brito et al., 1990). Chymotrypsin truncated R67 DHFR was prepared as described by Reece et al. (1991).

Gel Filtration. Gel filtration was carried out at 4 °C using a Pharmacia FPLC and a Superose HR16-50 column equilibrated in 50 mM MES–100 mM Tris–50 mM acetic acid–10 mM β-mercaptoethanol buffer (MTA). This buffering system maintains a constant ionic strength over the pH range 4.5–9.5 (Ellis & Morrison, 1982). The K_{av} of R67 DHFR (29 μM expressed as tetramer[3]) as a function of pH was monitored where K_{av} is (elution volume – void volume)/(total bed volume – void volume). Flow rate was 1 mL/min. A standard curve (pH 8) plotting the molecular weight of protein standards (Pharmacia LMW calibration kit) versus K_{av} allowed determination of the molecular weight of R67 DHFR.

Fluorescence. Protein fluorescence was monitored at 23 °C using a Perkin-Elmer LS-5B spectrometer. Tryptophan residues were excited at 295 nm (slit 10 nm), and emission was monitored at 350 nm (slit 5 nm). For pH titrations,

[2] A chymotrypsin-truncated form of R67 DHFR (Reece et al., 1991) has been crystallized in a tetrameric form (Narayana, Matthews, and Xuong, personal communication). Each monomer in the structure has electron density for residues 17–78. The amino acids in the first monomer are labeled 17–78; those in the second monomer, 117–178; in the third, 217–278; and in the fourth, 317–378. For brevity, when H62 is mentioned in the text, all four histidines (62, 162, 262, 362) are implied.

[3] All concentrations of R67 DHFR are expressed as tetramer, unless noted otherwise.

1.32–68.0 μM R67 DHFR in MTA polybuffer was titrated with small volumes of 2 M HCl (or 2 M NaOH). Cells with 1-, 0.4-, and 0.2-cm path lengths were used. After addition of acid, the solution was allowed to equilibrate for 1 min and the fluorescence and pH were monitored. pH measurements were performed directly in the fluorescence cuvettes using a microelectrode (Microelectrodes, Inc.).

The fluorescence of 8 μM R67 DHFR at pH 7 and 5 was quenched by adding aliquots of 5 M potassium iodide. Fluorescence emission of the protein solution and a D,L-tryptophan control was monitored at 340 nm. Data were fit to the Stern–Volmer equation

$$F_0/F = 1 + K_{SV}[Q] \quad (1)$$

where F_0 and F are the fluorescence intensities in the absence and presence of quencher, respectively, Q is the concentration of quencher, and K_{SV} is the Stern–Volmer quenching constant.

Diethyl Pyrocarbonate (DEPC) Modification. Stock solutions of DEPC were prepared by diluting DEPC with cold absolute ethanol. The concentration of stock DEPC was then calculated from the increase in absorbance at 240 nm upon addition to a solution of 10 mM *N*-acetylhistidine. An extinction coefficient of 3600 M^{-1} cm^{-1} was used (Holbrook & Ingram, 1973). Reaction mixtures contained ~170 μM R67 DHFR (tetramer) in 50 mM phosphate–1 mM EDTA buffer (pH 6.00) and a 5–10-fold molar excess of DEPC per monomer (i.e., 3.4–6.8 mM DEPC). The reaction was incubated at 22 °C for 1–1.5 h, and modification was monitored by loss of enzyme activity until ~10% activity remained. Excess DEPC was removed by passing the reaction mixture over a 1 × 25 cm G-25 Sephadex column. Modified protein was then separated from any unmodified protein by passing the protein mixture over an Affi-gel blue (Bio Rad) column (1–2 mL of resin) equilibrated in 10 mM phosphate–1 mM EDTA (pH 6) buffer. Native R67 DHFR binds to this column and can be eluted with buffer containing 0.1 M KCl.

The modified protein was treated with neutral hydroxylamine (0.375–0.875 M) at 4 °C to remove the *N*-carbethoxy group from histidine (Miles, 1977). Hydroxylamine did not affect the activity of control reactions.

The stoichiometry of the reaction was determined by modifying R67 DHFR with a 4–5 molar excess of ^{14}C-labeled DEPC (Sigma). Unreacted DEPC was removed by dialysis against 50 mM phosphate–1 mM EDTA buffer (pH 7). Radioactivity was monitored with a Beckman LS 3801 scintillation counter.

Kinetic Analysis. Steady-state kinetic data were obtained as previously described (Reece et al., 1991). Briefly, assays were performed at 30 °C in MTA Polybuffer. Both NADPH and dihydrofolate concentrations were varied at subsaturating levels to obtain k_{cat}, $K_{m(NADPH)}$ and $K_{m(DHF)}$ values. Enzyme addition initiated the assay.

Concentrations were determined spectrophotometrically using molar extinction coefficients of 28 000 M^{-1} cm^{-1} at 282 nm for DHF (Blakley, 1960) and 6220 M^{-1} cm^{-1} at 340 nm for NADPH (Horecker & Kornberg, 1948). The molar extinction coefficient for DHF utilization by DHFR was 12 300 M^{-1} cm^{-1} at 340 nm (Baccanari et al., 1975). Enzyme concentrations were initially determined using the biuret procedure (Gornall et al., 1949) and then routinely measured using an extinction coefficient of 1.825 mL mg^{-1} cm^{-1} at 280 nm.

Model Fitting. A model to describe the behavior of R67 DHFR as a function of pH is shown in Scheme I, where T and TH_{2n} are tetrameric and D and DH_n are dimeric forms

Scheme I

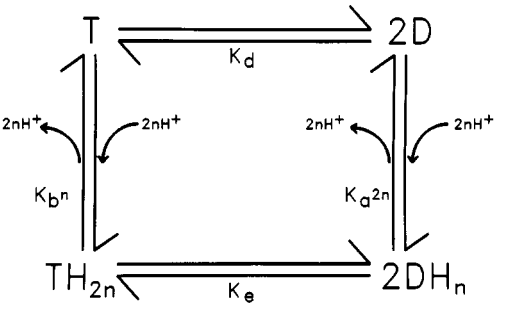

Scheme II

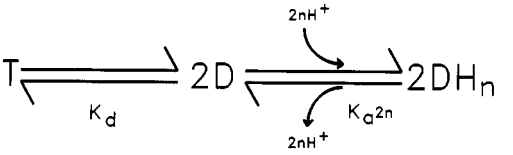

of unprotonated and protonated R67 DHFR, K_d and K_e are dissociation constants, and K_a and K_b are ionization constants. On the basis of the dimer structure and 222 symmetry element in Figure 1 and the values of kinetic pK_a's [5.8, Morrison and Sneddon (1990); ~5.5, Brito et al. (1990)] as well as our data presented below, the ionizing groups are His62, -162, -262, and -362. Addition of only one proton per dimer (n = 1) could occur if a hydrogen bond were to exist between two histidines at each of the two dimer–dimer interfaces. Alternatively, if no such hydrogen bond exists, two protons per dimer (n = 2) can be added.

In Scheme I, protons could potentially add to either tetrameric or dimeric R67 DHFR. However, our sedimentation equilibrium data at pH 5.01 and 8.01 (see below) suggest the K_e for formation of protonated tetramer is extremely high, i.e., ≥3.8 mM, in comparison to the K_d for formation of unprotonated tetramer (≤50 nM). Therefore, computer fitting of data has utilized Scheme II, an abbreviated version of Scheme I. Poe (1973) used a similar approach in simplifying linked dimerization and protonation reactions in NMR studies of folate.

From Scheme II, an equation can be derived for the concentration of D,

$$[D] = (K_d/4)\{-(1 + [H]^n/K_a^n) + [(1 + [H]^n/K_a^n)^2 + 8P_{tot}/K_d]^{1/2}\} \quad (2)$$

where P_{tot} describes the total protein concentration and equals $2T + D + DH_n$ and n describes the number of ionizations per dimer (1 or 2). For the case of n = 2 ($D \leftrightarrow DH \leftrightarrow DH_2$), we have assumed that DH does not accumulate and both ionizations have identical pK_a's.

The fraction of total dimer (F_{app}) equals $([D] + [DH_n])/P_{tot}$, where $[DH_n] = ([D][H]^n)/(P_{tot}K_a^n)$. The observed changes in fluorescence (F_{obs}) can be related to F_{app} by the equation

$$F_{app} = (F_{obs} - F_{tet})/(F_{di} - F_{tet}) \quad (3)$$

where F_{tet} and F_{di} are the calculated fluorescence values for tetramer and total dimer. We have assumed the fluorescence of D and DH_n is equivalent.

The above equations were combined into a single equation and experimental data fit to eq 4, where [D] is defined by eq

$$F_{obs} = \{(F_{di} - F_{tet})\{[D] + ([D][H]^n)/K_a^n\}/P_{tot}\} + F_{tet} \quad (4)$$

2. Since eq 4 predicts F_{obs} is dependent on P_{tot}, several data sets at different protein concentrations were collected and fit simultaneously (global analysis) with NONLIN. Simultaneous fitting of several correlated data sets allows estimation of two variables, K_d and K_a. NONLIN, the generous gift of Dr. Michael L. Johnson (University of Virginia), uses a modified Gauss–Newton algorithm in a nonlinear least-squares fitting procedure (Doyle et al., 1991; Johnson et al., 1976; Johnson & Fraser, 1985). Confidence intervals are correlated with other parameters and are asymmetric.

Finally, an abbreviated version of Scheme II,

$$T + 2nH^+ \overset{K_{overall}}{\leftrightarrow} 2\,DH_n$$

was used to generate eq 5 and fit the K_{av} data from molecular sieving experiments:

$$K_{av_{obs}} = \{(K_{av_{di}} - K_{av_{tet}})\,\{[H]^{2n}/(4K_{overall}P_{tot})\} \times \{-1 + [1 + (8K_{overall}P_{tot}/[H]^{2n})]^{1/2}\}\} + K_{av_{tet}} \quad (5)$$

where $K_{overall} = ([T][H]^{2n})/[DH_n]^2 = K_a^{2n}/K_d$ in units of M or M^3 for $n = 1$ or 2, respectively, $K_{av_{obs}}$ is the observed K_{av}, and $K_{av_{tet}}$ and $K_{av_{di}}$ are calculated values for tetramer and dimer. This fit was performed with a nonlinear least-squares fitting program (NLIN) in the Statistical Analysis Systems program package (Sas Institute Inc., Cary, NC).

Sedimentation Equilibrium. Sedimentation equilibrium experiments were performed at ~20 °C with a Beckman-Spinco Model E ultracentrifuge equipped with a photoelectric scanner and temperature control system. Data at 280 nm were collected using the scanner after equilibrium was attained (usually between 24 and 30 h) by means of a DAS-8PGA analog to digital interface (Metrabyte) to a Compaq 386SX personal computer in the form of voltage versus radius. Prior to analysis, the data were converted to absorbance versus radius by a standardized calibration of voltage to absorbance. Double sector cells with charcoal-filled epon centerpieces and quartz windows were used in a four-hole, An-F Ti rotor. Solvent densities at the different pH values were determined pychnometrically.

The molecular weight and partial specific volume of R67 DHFR are known from the nucleotide sequence of the structural gene and are 8430 Da/chain and 0.7159 mL/g, respectively (Brisson & Hohn, 1984). The data from sedimentation equilibrium were analyzed either in terms of a single homogeneous species or in terms of a model where tetrameric R67 DHFR was in reversible equilibrium with dimers. For a single species model, data were fit according to

$$c_r = B + c_m \exp[M(1 - v\rho)\omega^2(r^2 - r_m^2)/2RT] \quad (6)$$

where c_r is the concentration of a monodisperse protein at radial position, c_m is the concentration of the species at a reference position (i.e., the meniscus), M is the molecular weight, v is the partial specific volume, ρ is the solvent density, ω is the angular velocity, r is the radial distance in centimeters from the center of rotation, r_m is the distance in centimeters from the center of rotation to the meniscus, R is the gas constant, T is the temperature, and B is a correction term for a nonzero baseline.

At pH values where analysis in terms of a single species was inadequate, data were alternatively fit to

$$c_r = B + c_{m,D} \exp[M_D(1 - v\rho)\omega^2(r^2 - r_m^2)/2RT] + (c_{m,D})^2/K_{42} \exp[M_T(1 - v\rho)\omega^2(r^2 - r_m^2)/2RT] \quad (7)$$

where $c_{m,D}$ is the concentration of the dimeric species at the reference position, M_d and M_T are dimer and tetramer molecular weights, and K_{42} measures $[DH_n + D]^2/[T + TH_n]$, i.e., total dimer[2] and tetramer concentrations. Using Scheme II, K_{42} can be converted into a K_d value if values for n and pK_a are assumed as $K_{42} = K_d(1 + [H]^n/K_a^n)^2$.

Analysis of the data was performed using nonlinear least-squares analysis (Johnson & Fraser, 1985). Data at all pH values were analyzed using both eqs 6 and 7 to determine the best fit. The equilibrium data fit to eq 6 yielded values for molecular weight and the concentration at the reference position. Data analyzed using eq 7 yielded values for the concentration of dimer at the interface position and the natural logarithms of K_{42}. (Since K_{42} is directly proportional to the free energy for dimer–tetramer assembly, the confidence interval for this parameter is also more accurately described using units of free energy rather than units of molecules per liter). In these analyses it was implicitly assumed that both dimeric and tetrameric species had identical specific extinction coefficients and partial specific volumes. In all cases, data for two different initial concentrations were analyzed simultaneously as a test for homogeneity and reversibility of the dimer–tetramer equilibrium (Roark, 1976) and to constrain confidence intervals for the parameter values (Johnson & Fraser, 1985).

Proton NMR. Proton NMR spectra were obtained at 600.13 MHz on a Bruker AM600 spectrometer, equipped with an Aspect 3000 computer. Data were collected at 283 K, as determined by a methanol thermometer. The sample was placed in a 5-mm tube, and an external reference consisting of 1 mM sodium 3-(trimethylsilyl)propionate-*2,2,3,3-d*$_4$ (TSP, shift reference) and 2 mM tyrosine methyl ester (intensity reference) in ^2H_2O was placed in a 2-mm coaxial tube. Water presaturation was performed during the initial relaxation delay (0.38 s). Data were collected under the following conditions: sweep width, 11 ppm (6579 Hz); pulse width, 5 μs (75°); recycle time, 1.0 s; number of scans, 2000 (pH* 4.28–6.28) to 5000 (pH* 6.62–7.04). Line broadening of 0.1 Hz was applied to each FID prior to Fourier transformation. A linear baseline correction was applied to each spectrum.

R67 DHFR that had been lyophilized from ^2H_2O solution was reconstituted in 1 mL of ^2H_2O containing 0.1 M potassium phosphate–5 mM EDTA (pH* 7.3) to a final DHFR concentration of 1.40 mM tetramer. pH readings were obtained with a glass microelectrode and were not adjusted for D_2O content, because of opposing effects of D_2O on the meter readings and on dissociation constants. Uncorrected pH readings are denoted pH*. To adjust the pH*, the sample was transferred to a micro reaction vessel at 0–5 °C fitted with a magnetic stir bar (Pierce, Rockford, IL) and a small volume (4–30 μL) of 0.1 and 0.5 M NaOD or DCl was added. The sample was temperature equilibrated for 20 min in the spectrometer before data acquisition. Intensity data were corrected for dilution and losses during the titration procedure (see below).

An incomplete titration curve describing chemical shifts for the C2 proton of H62 was fit to the following equation:

$$(\delta_{H^+} - \delta_{obs})/(\delta_{H^+} - \delta_{Ho}) = K_a^n/(K_a^n + [H^+]^n) \quad (8)$$

where δ_{obs} is the observed chemical shift, δ_{H^+} and δ_{Ho} are the calculated chemical shifts for protonated and unprotonated H62, and n measures cooperativity between titrations (Markley, 1975).

The relative intensity of the sharp C2 proton peak was determined initially by dividing the peak area for the sharp C2 proton of H62 by the area of an unidentified peak at approximately 8.42 ppm. The area of the latter peak does not appear to change during pH* titrations. Peak areas were determined by weight. The variation in peak intensity as a function of pH* was fit to eq 5, yielding values for $K_{overall}$ and n. Enzyme concentration was entered as a third variable to correct for dilution of sample by acid or base additions. Qualitatively similar fits with smaller errors were then determined using the ratio of peak height for the sharp H62 C2 proton peak to two or more of the aromatic protons of 2 mM tyrosine methyl ester contained in a capillary. The latter values are reported below.

To determine the number of protons associated with the H62 peak at low pH*, the intensity of the sharp H62 C2 proton peak was quantified by comparison to the resonances of controlled concentrations of $NADP^+$. At low pH*, $NADP^+$ does not bind to R67 DHFR.

RESULTS

Gel Filtration. To investigate whether the titration seen in kinetic pH profiles could be associated with ionization of histidine(s), the elution pattern of R67 DHFR from a molecular sieving column was analyzed. At pH 5, R67 DHFR elutes from an FPLC Superose 12 column as a dimer, and at pH 8.0, it elutes as a tetramer.[4] At intermediate pH values, the protein elutes at an average position corresponding to the percent tetramer and dimer present. The average elution position indicates tetramer and dimer are in rapid equilibrium.

A plot of K_{av} versus pH depicts a titration in molecular weight (Figure 2). A 30-fold dilution of protein concentration by the chromatography step was estimated, and the best fit of the data to eq 5 yields a $K_{overall}$ of $3.65 \times 10^{-7} \pm 4.38 \times 10^{-8}$ M when $n = 1$. From Scheme II, $K_{overall} = K_a^{2n}/K_d$. The values for limiting K_{av}'s at low and high pH values are 0.468 ± 0.0022 and 0.344 ± 0.0015. These values correspond to molecular weights of 24 000 and 42 000, respectively, a 1.8-fold difference. The amino acid sequence predicts molecular weights of 16 860 and 33 720 for dimeric and tetrameric R67 DHFR. Aberrant molecular weight estimates determined by gel filtration are not unusual, however, as the shape of the molecule as well as the size affects elution (Potschka, 1987).

Also shown in Figure 2 are the residuals for the $n = 1$ and $n = 2$ fits. For $n = 2$, the theoretical curve predicts a steeper slope than the data actually possesses. The residuals for $n = 1$ display a more random pattern and thus a better fit.

Fluorescence of R67 DHFR. There are two tryptophans per R67 DHFR monomer. One tryptophan (45) in β-strand B is buried at the monomer–monomer interface in dimeric R67 DHFR (Matthews et al., 1986; Reece et al., 1991).

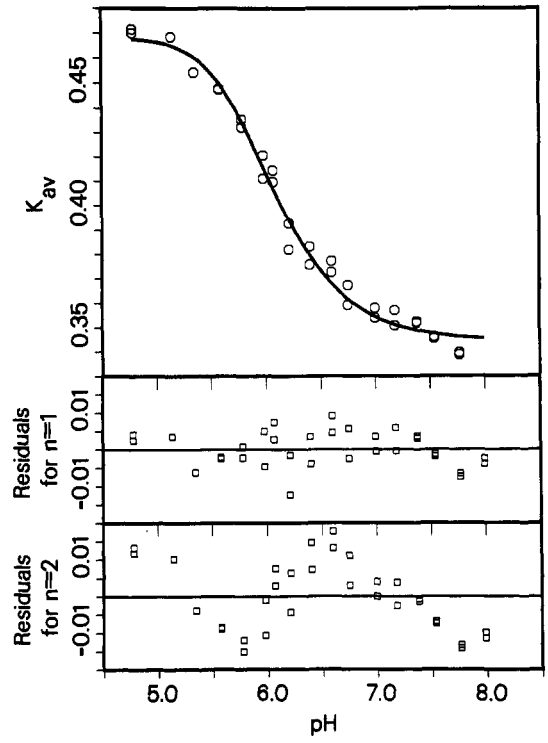

FIGURE 2: Titration of K_{av} in R67 DHFR as a function of pH. R67 DHFR (29 μM) was applied to a HR16-50 molecular sieving column and the elution position monitored from pH 5 to 8. Duplicate points are shown. A 30-fold dilution of protein concentration by the chromatography step was estimated. The theoretical curve shown was generated by nonlinear fitting to eq 5 and best-fit values are noted in the text. Plots of the residuals (difference between actual and predicted data points) for $n = 1$ and 2 are shown.

Another tryptophan (38) occurs at the dimer–dimer interface near His 62 in dimeric R67 DHFR (see Figure 1). The fluorescence of W38, -138, -238, and -338 should be sensitive to alterations in the tetramer–dimer equilibrium if W38 moves from a hydrophobic (tetramer) to a hydrophilic environment (dimer). Additionally, the ionization state of histidine could affect the fluorescence of nearby tryptophans (Loewenthal et al., 1991). When the fluorescence emission spectrum of R67 DHFR at pH 5 is compared to that at pH 8 (Figure 3A), a blue shift of the emission maximum is displayed.

This blue shift allows us to monitor a titration in R67 DHFR fluorescence as a function of pH (Figure 3B). Since association of two protonated dimers into tetrameric R67 DHFR is a bimolecular reaction, a protein concentration dependence of this titration is predicted by eq 4. Therefore, titrations for three different protein concentrations are shown in Figure 3B. All three data sets were combined in a single curve-fitting procedure (global analysis) to resolve the model parameters K_a and K_d in Scheme II. The best-fit values ($n = 2$) are $K_d = 9.72$ nM (5.43–12.9 nM, 95% confidfence interval) and $pK_a = 6.84$ (6.79–6.92, 95% confidence interval). The individual fluorescence limits for each concentration were concurrently fit and then converted to F_{app} (eq 3) to facilitate comparison.

Also shown in Figure 3B are the residuals for the $n = 2$ and $n = 1$ fits. The residuals for $n = 1$ are clearly nonrandom while the residuals for $n = 2$ display a more random pattern and thus a better fit.

Iodide Quenching. Iodide is a large, polar anion that efficiently quenches the fluorescence of surface tryptophan residues (Kurzban et al., 1989; Lakowicz, 1983; Eftink & Ghiron, 1981). As shown in Figure 4, quenching of R67

[4] Partial unfolding of tetrameric R67 DHFR at low pH was initially considered as a model to fit the sieving data. However, a comparison of circular dichroism spectra at pH 5 and 7 indicates only subtle alterations in structure (data not shown). In addition, equilibrium unfolding studies of 12 μM R67 DHFR at pH 5.0 indicate unfolding does not occur until 1–1.5 M guanidine hydrochloride is added (Reece et al., 1991). Finally, the K_{av} values in DEPC-modified R67 DHFR do not show a pH titration, consistent with stabilization of dimeric R67 DHFR by DEPC modification (see below). Therefore the partial unfolding model was rejected.

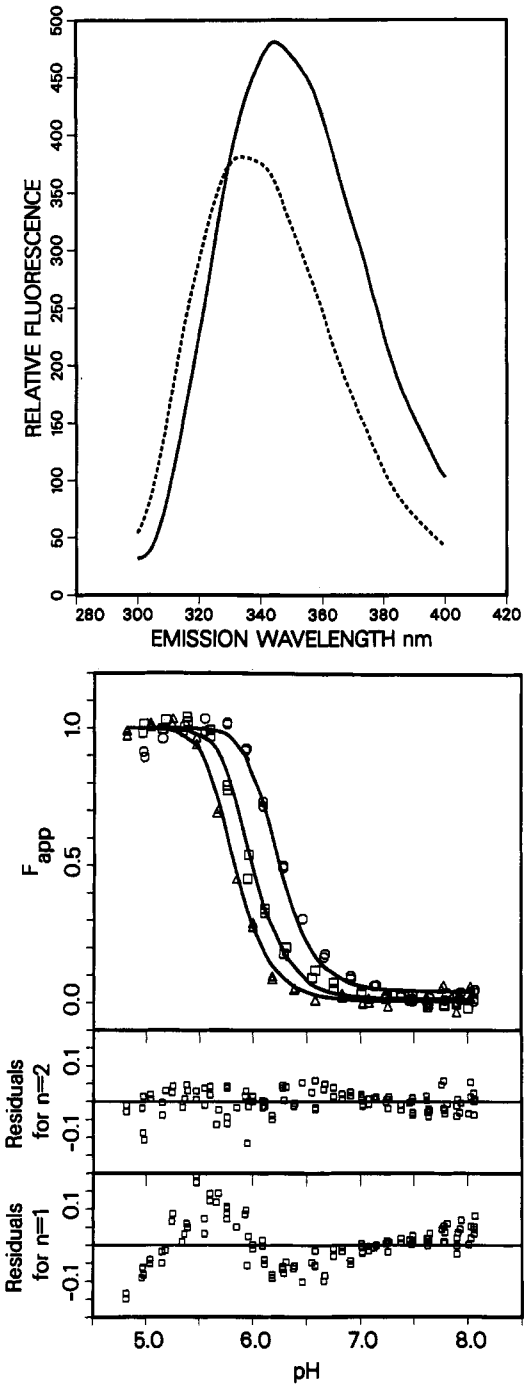

FIGURE 3: (A) Fluorescence emission spectra of 1.3 μM R67 DHFR (excitation 295 nm). The solid line describes emission at pH 5.0 and the dashed line emission at pH 8.06. Additional conditions are described under Materials and Methods. (B) R67 DHFR fluorescence at 350 nm monitored as a function of pH. Three different protein concentrations were used: 1.31 (○), 12.3 (□), and 55.6 μM (△). Standard errors in fluorescence and pH were ≤5% and ≤7%, respectively. The data were converted to F_{app} (eq 3) to facilitate comparison. The theoretical curves shown were generated by nonlinear fitting to eq 4 and best-fit values are noted in the text. A plot of the residuals for $n = 1$ and $n = 2$ are shown.

DHFR fluorescence by iodide at pH 5.0 occurs to a substantial degree ($K_{SV} = 1.53 \times 10^{-3}$ M^{-1}), while at pH 7.0, quenching is essentially zero (i.e., K_{SV} is slightly negative, -7.11×10^{-5} M^{-1}). Quenching of D,L-tryptophan was highly efficient at both pH values (pH 7 not shown). According to Scheme II and Figure 1, tryptophans 38, 138, 238, and 338 should be accessible to iodide quenching at pH 5.0 (dimeric R67 DHFR); however, at pH 7.0, they should be inaccessible (tetrameric

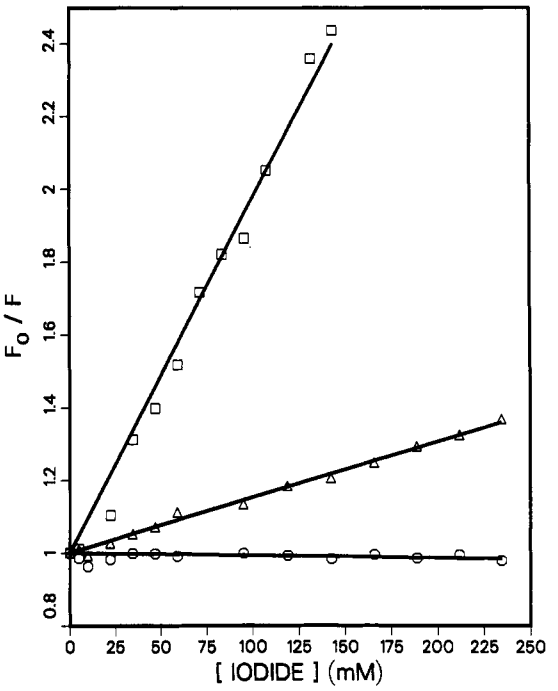

FIGURE 4: Quenching of R67 DHFR fluorescence (excitation 290 nm) by potassium iodide. The fluorescence of 8 μM R67 DHFR was evaluated at pH 5.0 (△) and 7.0 (○) and the effect of KI addition noted. F_0 and F are the fluorescence intensities in the absence and presence of KI. Quenching of a D,L-tryptophan control at pH 5.0 is shown (□).

R67 DHFR). The observed iodide quenching results are consistent with this model. From the dimeric crystal structure, Trp45 should remain buried in both dimer and tetramer environments.

Sedimentation Equilibrium. The molecular weight of R67 DHFR was investigated by sedimentation equilibrium as a function of pH. At pH 8.01, two different initial concentrations of protein distribute at sedimentation equilibrium as shown in Figure 5A. Attempts to analyze the data in terms of a T ↔ 2D equilibrium indicated that no unique fit could be obtained unless a dissociation constant of 50 nM or less was assumed. Although this assumption allows for a random distribution of residuals versus radius, as seen in Figure 5C, it is unjustified since, even at the lowest protein concentrations accessible in this measurement, no significant concentration of dimers were detected. Alternatively, the data of Figure 5A were analyzed in terms of eq 6 to yield a molecular weight of 33 000, with 67% confidence intervals of 32 600–33 400 Da. This small confidence interval, the random distribution of the residual error versus radius (Figure 5B), the smaller value for the sum of the residuals squared than obtained for the fit to the more complex model (eq 7), and the reasonable agreement with the molecular weight predicted from the nucleotide sequence are most simply interpreted in terms of a stable tetrameric quaternary structure for R67 DHFR at elevated pH.

At pH 5.01, two other concentrations of R67 DHFR were brought to sedimentation equilibrium, as shown in Figure 5D. These data were analyzed in terms of a model involving a $TH_{2n} \leftrightarrow 2DH_n$ equilibrium as described in eq 7, with the distribution of the residuals from the fit presented in Figure 5E. This analysis yielded a dissociation constant for the dimer–tetramer equilibrium of 3.8 mM (K_e in Scheme I). An alternative analysis for a single species yielded a molecular weight of 16 700 with 67% confidence intervals of 16 500–16 900 Da. This fit yielded a random distribution of residuals,

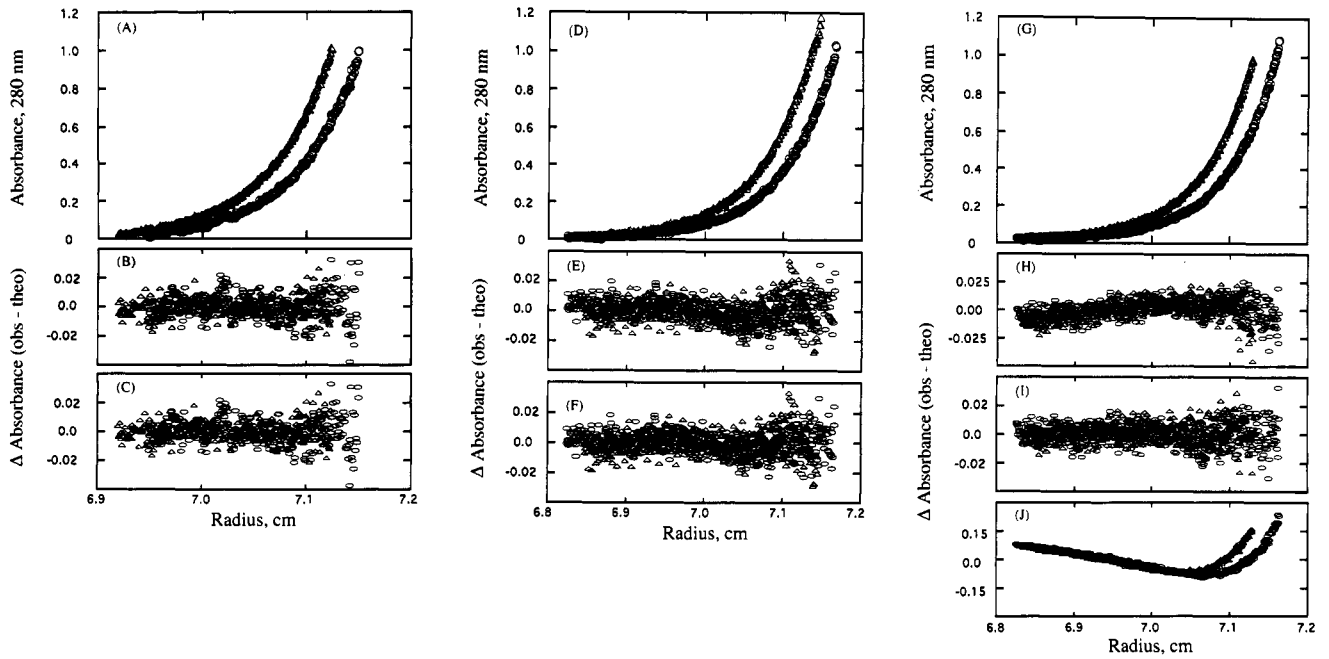

FIGURE 5: Sedimentation equilibrium of R67 DHFR in MTA buffer. Data in the form of absorbance versus radius from the center of rotation were obtained as described under Materials and Methods. (A) At pH 8.01, two different initial concentrations were used to test for homogeneity: 0.28 (Δ) and 0.14 mg/mL R67 DHFR (O). The rotor speed was 24 048 rpm and the temperature 21.5 °C. Lower panels: (B) residual error as a function of radial distance from the center of rotation for analysis of both distributions simultaneously fit to a single monodisperse species as described in eq 6; (C) residuals associated with a fit of the data to eq 7 describing a T ↔ 2D equilibrium. A K_d of 50 nM was assumed in order to be able to fit the data. (D) At pH 5.01, two different initial concentrations were used: 0.23 (Δ) and 0.11 mg/mL R67 DHFR (O). The rotor speed was 32 049 rpm and the temperature 22.1 °C. Lower panels: (E) residual error from fitting the data to eq 7 describing a TH_{2n} ↔ $2DH_n$ equilibrium using an assumed K_e of 3.8 mM; (F) residuals from fitting the data to a monodisperse species as described in eq 6. (G) At pH 6.50, 0.26 (Δ) and 0.12 mg/mL R67 DHFR (O) were used. The rotor speed was 23 933 rpm and the temperature was 20.0 °C. Lower panels: (H) residuals from fitting the data to a monodisperse tetramer (eq 6); (I) an equilibrium between T ↔ 2D described by eq 7; (J) a monodisperse dimer (eq 6). Best-fit values are given in the text.

presented in Figure 5F, and a smaller sum of residuals squared than obtained for the more complex model. These results suggest that the value of 3.8 mM can be considered a lower limit for the protonated dimer–protonated tetramer equilibrium since, at this pH, the enzyme is most simply described as a dimer.

At intermediate pH values of 5.81, 6.13, and 6.50, the concentration distribution of two samples of R67 DHFR could not be uniquely fit by a model describing the sedimentation of a single, monodisperse species. Therefore the data were analyzed in terms of eq 7, yielding equilibrium dissociation constants (K_{42}) for the dimer–tetramer equilibrium of 10 300 (9 640–11 000, 67% confidence interval), 3510 (3230–3820), and 360 (317–412) nM at pH 5.81, 6.13, and 6.50, respectively. Data collected at pH 6.5 are displayed in Figure 5G. K_{42} describes $[D + DH_n]^2/[T + TH_n]$, which can be converted to the K_d described in Scheme II, if values for pK_a and n are assumed. Several values for K_d are calculated and listed in Table I.

Residuals associated with fitting the data at pH 6.5 to eq 6 describing either a monodisperse tetramer or a monodisperse dimer are shown in Figure 5H and J, respectively. Nonrandom distributions indicate a poor fit.

A slope of $2n$ is predicted for a plot of pH versus $-\log 1/K_{42}$ (Wyman, 1964). Best fits using data from pH values 5.81, 6.13, and 6.50 yield $2n = 2.12 \pm 0.323$, indicating $n = 1.06$.

NMR. To confirm that H62 is ionizing in this pH range, proton NMR spectra were obtained at various pH*. The peaks associated with histidine were first identified by a change in chemical shift induced by DEPC modification at pH* 5.78 [Figure 6A; Smith and Mildvan (1981)]. The 8.4 ppm peak that moved upfield to 8.1 ppm upon addition of DEPC was assigned to the C2 proton of H62. Similarly, the peak at 7.0 ppm that moved downfield to 7.2 ppm upon modification was assigned to C4 of H62. These two resonances returned to premodification values after hydroxylamine treatment.

Inspection of the NMR spectra (Figure 6B) reveals that (a) when the pH* is raised, both C2 and C4 resonances shift upfield without appreciable changes in line width, suggesting protonated and unprotonated forms of H62 in dimeric R67 DHFR are in rapid equilibrium, and (b) these C2 and C4 peak intensities diminish at high pH*. These sharp resonances observed at low pH* indicate H62 is highly mobile, consistent with the crystal structure of dimeric R67 DHFR. At high pH, a peak at ~7.35 ppm appears. The intensity of this peak increases with pH, reaching a maximum at pH ~7.0. At this pH, the sharp C2 resonance is not observed. We propose the 7.35 ppm resonance describes the C2 proton of H62 in a tetrameric environment. The chemical shift of this peak does not shift with pH, suggesting that histidine in a tetrameric environment is fully deprotonated and that tetramer and dimers are in slow equilibrium on the NMR time scale. Preliminary NOE and COSY cross-peak data are consistent with the 7.35 ppm peak being the C2 proton of H62 in tetrameric R67 DHFR. However, a more rigorous NMR experiment using isotopically labeled protein is underway to confirm this interpretation.

Figure 6C shows the pH* profile of the chemical shift for the sharp C2 resonance of H62 (dimeric R67 DHFR). Best-fit values to eq 8 for this incomplete titration curve are $n = 1$, p$K_a = 6.77 \pm 0.043$, $\delta_{H^+} = 8.61 \pm 0.0014$, $\delta_{H_o} = 7.99 \pm 0.039$. According to Markley (1975), n in eq 8 measures cooperativity between titrations; also a 0.62 ppm change in chemical shift is within the normal range for histidine ionizations. The pK_a value and its error are misleading since fitting is dependent on the last point entered; i.e., the pH*

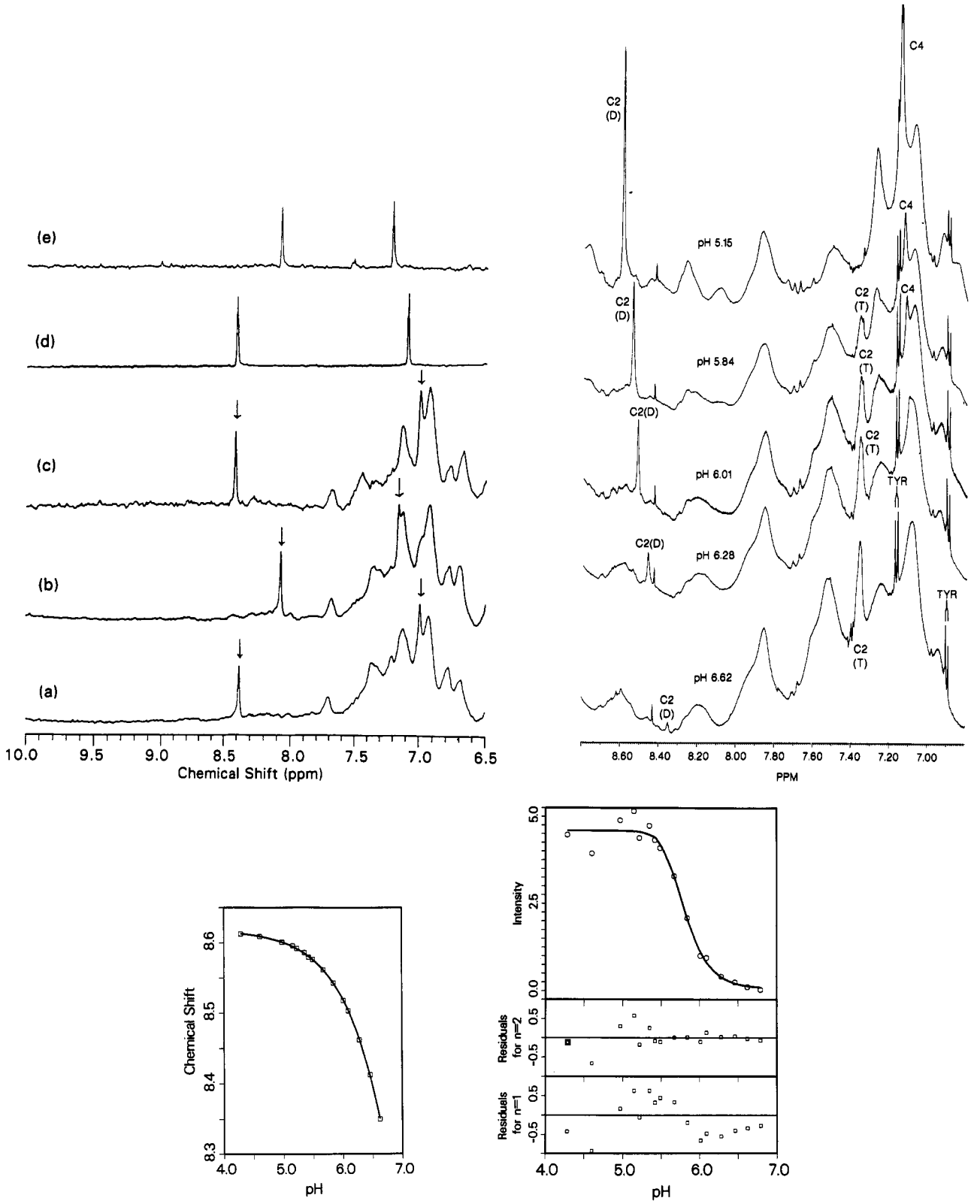

FIGURE 6: (A, upper left) Spectra of (a) 0.45 mM native R67 DHFR in 50 mM phosphate buffer (pH* 5.78), (b) R67 DHFR after treatment with 7.5 mM DEPC, (c) DEPC modified R67 DHFR after treatment with 15 mM hydroxylamine, (d) 1.1 mM *N*-α-acetyl-L-histidine in 50 mM phosphate buffer (pH* 5.70), and (e) *N*-α-acetyl-L-histidine treated with 1.2 equiv of DEPC. The C2 (~8.4 ppm) and C4 (~7.0 ppm) protons of H62 are indicated by arrows. This set of spectra was obtained at room temperature. (B, upper right) Representative proton NMR scans at pH* 5.15, 5.84, 6.01, 6.28, and 6.62. The sharp C2 proton peak of H62 in dimeric R67 DHFR is indicated at 8.3–8.6 ppm; the broader peak proposed for the C2 proton of H62 in tetrameric R67 DHFR is shown at ~7.35 ppm; the C4 proton peak of H62 is indicated at ~7.18 ppm; the unidentified peak at ~8.42 ppm was used for initial peak intensity calculations; and the aromatic resonances of an internal marker, tyrosine methyl ester, are indicated at 6.9 and 7.15–7.20 ppm. (C, lower left) The chemical shift of the sharp C2 proton of H62 as a function of pH*. The curve was fit to eq 8 and best-fit values are noted in the text. (D, lower right) A ratio of sharp peak intensities for the C2 proton of H62 in dimeric R67 DHFR to two or more of the aromatic peaks of tyrosine methyl ester was plotted as a function of pH*. The curve was fit to eq 5 ($n = 2$), and best-fit values are given in the text.

Table I: Comparison of Best-Fit Values from the Various Techniques Used To Study the $T \leftrightarrow 2D + 2nH^+ \leftrightarrow 2DH_n$ Equilibrium

technique	$K_{overall}$[a] (K_a^{2n}/K_d)	pK_a	K_d, nM	n
molecular sieving	3.65×10^{-7}			1
fluorescence	4.49×10^{-20}	6.84	9.72	2
NMR	3.17×10^{-21} [b]	≥6.77[c]	≤262	2[b]
sedimntn equilib				
at pH 8.01			≤50	
at pH 5.81	2.78×10^{-7}	6.84 (assumed)	75.0[d]	1
	2.86×10^{-7}	6.77 (assumed)	101[d]	1
at pH 6.13	2.23×10^{-7}	6.84 (assumed)	93.4[d]	1
	2.36×10^{-7}	6.77 (assumed)	122[d]	1
at pH 6.50	5.90×10^{-7}	6.84 (assumed)	35.4[d]	1
	6.55×10^{-7}	6.77 (assumed)	44.0[d]	1

[a] Units on $K_{overall}$ are M or M^3 for $n = 1$ and 2, respectively. [b] Calculated from the sharp peak intensity data (C2 proton of H62 in dimeric R67 DHFR; Figure 6d). [c] Calculated from chemical shift data (Figure 6c). [d] Calculated from $K_{42} = [D_{total}]^2/[T_{total}]$. From Scheme II, $K_{42} = K_d(1 + [H]^n/K_a^n)^2$. Assumed p$K_a$ values are listed.

profile is incomplete. This suggests the pK_a is ≥6.77.

A pH* profile depicting the intensities of the sharp C2 proton peak is shown in Figure 6D. The sharp C2 proton peak intensities have been proposed to monitor the environment of histidine in dimeric R67 DHFR. Fitting of the sharp peak intensity data to eq 5[5] yielded best-fit values of $n = 2$, $K_{overall} = 3.17 \times 10^{-21} \pm 2.00 \times 10^{-23}$ M^3, an upper intensity limit of 4.59 ± 0.109, and a lower intensity limit of 0.0688 ± 0.143. The residuals from nonlinear fits using $n = 1$ and 2 are shown.

To quantitate the number of protons associated with H62 in dimeric R67 DHFR at pH* 5.0, the sharp C2 proton peak was integrated and the number of protons counted using $NADP^+$ resonances as internal standards. Two protons were found, indicating R67 DHFR is a fully protonated dimer at low pH*.

Comparison of Best Fits Obtained from Various Techniques. A comparison of the various values for $K_{overall}$, K_a, K_d, and n obtained using various experimental approaches is summarized in Table I. Since the molecular sieving data (Figure 2) were collected at one protein concentration, only values for n and $K_{overall}$ could be estimated. Fluorescence data were collected for three different protein concentrations (Figure 3b); thus a global fit yielded values for n, K_a, and K_d. Proton NMR yielded chemical shift data (Figure 6C) permitting estimation of K_a. In addition, fitting of NMR intensity data for the sharp C2 proton peak of H62 to eq 5 yielded values for n and $K_{overall}$. Sedimentation equilibrium at pH extremes 5.01 and 8.01 allowed estimation of the limits for K_d and K_e directly (Scheme I), but at intermediate pH values, a bulk distribution of dimer–tetramer only is determined. A plot of pH versus $-\log 1/K_{42}$ indicates $n = 1$. If an estimate for pK_a is assumed, then a K_d can be calculated. When all these estimates are compared in Table I, it becomes obvious that we cannot accurately determine n. However, the pK_a estimates from fluorescence and NMR techniques are quite close while the K_d values diverge 27-fold. The highest K_d value is calculated from the NMR data using $K_{overall} = K_a^{2n}/K_d$ and a pK_a of 6.77. If this pK_a were higher, the K_d estimate would decrease. Considering these four very different techniques, the values for K_d and K_a are reasonably consistent, supporting our model presented in Scheme II.

[5] In addition, global fitting of two sets of peak intensity data for the C2 proton of H62 (sharp peak in dimeric R67 DHFR and 7.35 ppm peak in tetrameric R67 DHFR) along with the chemical shift data was performed to determine whether values for K_d and K_a could be extracted. Only one protein concentration was used since a direct measure of the pK_a should be provided by the chemical shift data and a direct measure of K_d should be provided by both sets of the intensity data. The chemical shift data were fit to eq 8; the sharp C2 proton peak intensity data (dimer) were concurrently fit to eq 4; and the 7.35 ppm C2 proton peak intensity data (tetramer) were concurrently fit to $Int_{obs} = (Int_{tet1} - Int_{tet2})([T]/P_{tot}) + Int_{tet2}$ (eq 9), where $[T] = [D]^2/K_d$, D is defined by eq 2, and Int_{tet1} and Int_{tet2} are the calculated upper and lower limits for tetramer C2 proton peak intensity. However, the global fits were sensitive to the initial pK_a and δ_{H_0} guesses and the error ranges were large. The nonunique fits resulted because two data sets (chemical shift, Figure 6c and tetramer C2 peak intensity) were incomplete. For the latter data set, the C2 proton peak intensities of H62 in tetrameric R7 DHFR were difficult to calculate at intermediate–low pH values as the 7.35 ppm peak disappeared under other protein peaks (see Figure 6b). The global fits have therefore not been presented although the ranges of pK_a, K_d, and δ_{H_0} values obtained were consistent with the other estimates of K_d and K_a presented in this paper.

Table II: Modification of R67 DHFR by Diethyl Pyrocarbonate (DEPC)

reagent excess per monomer	% activ remaining (after time t, min)	[hydroxylamine], M (time, h)	% reactivn
1.0	30 (97)	0.2 (1.5)	100
4.5	1.98 (60)	0.33 (12)	100
7.3	0.05 (150)	0.875 (22)	31
10.3	0.01 (135)	0.875 (22)	27

Modification of R67 DHFR by Diethyl Pyrocarbonate (DEPC). From the above data, we anticipated that modification of histidines 62, 162, 262, and 362 would disrupt the dimer–dimer interface and destabilize the tetramer. This would allow us to assess the activity of dimeric R67 DHFR. Therefore, histidines were modified by treatment with low levels of diethyl pyrocarbonate. Table II correlates DEPC levels with remaining activity. Since DEPC can also modify free amines, tyrosines, cysteines, lysines, and arginines, care was taken that enzyme activity could be fully restored by treatment with neutral hydroxylamine. This allowed us to find a DEPC concentration that selectively modified histidines as modification of other groups is not reversible upon hydroxylamine treatment (Miles, 1977; Lundblad & Noyes, 1984). Histidine modification was also evident from increases in absorbance at 240 nm while tyrosine or tryptophan modification was not evident from changes in absorbance around 280 nm (Miles, 1977).

After treatment with DEPC at a 1:1 DEPC:monomer ratio, the ability of the modified protein to form a tetramer was evaluated. Modified R67 DHFR elutes from a Superose 12 column as a doublet at pH 8.0. The major peak has a K_{av} value (0.435) corresponding to a dimer and a minor peak with a K_{av} corresponding to a tetramer. Again, native R67 DHFR elutes as a tetramer ($K_{av} = 0.340$) at this pH. Additionally, native R67 DHFR binds to folate (Salter et al., 1972) and Affi-gel blue (Cibacron blue dye) affinity columns and is eluted by addition of 0.1 M KCl to the buffer. In contrast, the majority of DEPC-modified protein does not bind to either column. Cibacron blue dyes have been proposed to bind to nucleotide binding folds in numerous enzymes.

To determine if any activity is associated with modified, dimeric R67 DHFR, DEPC (at a 5:1 ratio) and any unreacted (or hydrolyzed) tetramer were removed by passing the protein mix over a G-25 column once and over an Affi-gel blue column twice. The activity was then immediately assayed at pH 7.0, and both dihydrofolate and NADPH concentrations varied.

Values for k_{cat}, $K_{m(NADPH)}$ and $K_{m(DHF)}$ were 0.052 ± 0.007 s^{-1}, 72 ± 5.5 μM, and 40 ± 4.0 μM, respectively. These values represent the *upper* limits for activity of dimeric R67 DHFR and suggest that modified dimer is at least 200–600-fold less efficient (k_{cat}/K_m) than tetramer. For comparison, k_{cat}, $K_{m(NADPH)}$, and $K_{m(DHF)}$ values for tetrameric R67 DHFR are 1.3 s^{-1}, 3.0 μM, and 5.8 μM, respectively (Reece et al., 1991). Our qualifications on these values being upper activity limits arise because our [^{14}C]DEPC labeling data (below) indicate only 2.7 histidines/tetramer are labeled. Thus, partially modified dimers are probably present and may still be able to associate poorly and be marginally active. Alternatively, small amounts of unmodified tetrameric R67 DHFR may still be present due to either incomplete removal of tetramer by the affinity chromatography step or by hydrolysis of the modified histidine groups (Miles, 1977). The latter seems unlikely as the observed K_m values are 7–24-fold higher than normal.

To determine the stoichiometry of carbethoxy labeling, a 5-fold excess of ^{14}C-labeled DEPC was used. A total of 6.6 residues/tetramer were labeled at this ratio, and after hydroxylamine treatment, 3.9 residues/tetramer remained labeled (three different experiments). These results suggest only 2.7 histidines/tetramer were labeled and that 3.9 other residues were labeled. Modification at the second site does not affect enzyme activity. The N-terminal amino group or the side chain of Arg3 seemed reasonable candidates for the other modification site. Therefore the enzyme was modified with [^{14}C]DEPC, treated with hydroxylamine, and then truncated with chymotrypsin. Chymotrypsin has been found to cut R67 DHFR uniquely after Phe16, and the truncated enzyme retains full activity (Reece et al., 1991). The β-barrel structure of the enzyme is not affected as only the disordered N-terminus is removed by chymotrypsin treatment (Matthews et al., 1986). Polyacrylamide gel electrophoresis of R67 DHFR (Figure 7) shows the modified, hydroxylamine-treated native protein is radioactive but the chymotrypsin-treated enzyme is not. Thus, the additional DEPC modification sites occur in the N-terminal sequence.

To increase the number of histidines modified per tetramer, a higher DEPC level would be needed. However, as indicated in Table II, modification by a higher DEPC ratio is accompanied by incomplete removal of the carbethoxy group by hydroxylamine treatment, suggesting either modification of other groups essential for enzyme activity or disubstitution at histidine (Miles, 1977).

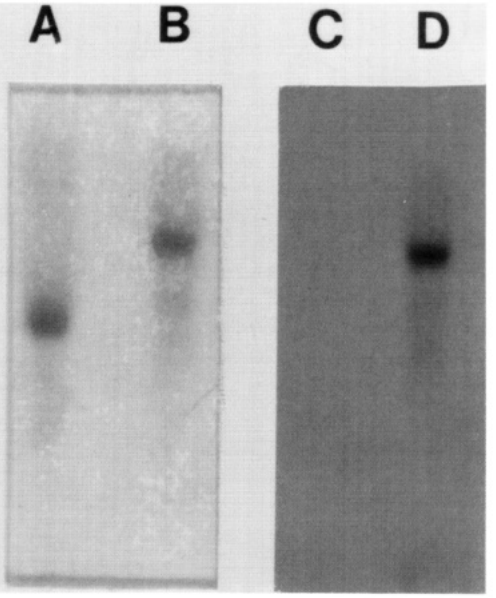

FIGURE 7: Nondenaturing polyacrylamide gel of native and chymotrypsin-truncated R67 DHFR. The protein was treated with [^{14}C]-DEPC and then with hydroxylamine. The fully reactivated protein was dialyzed and treated with chymotrypsin to truncate the N-terminal 16 residues. Truncated DHFR was dialyzed prior to electrophoresis. Protein concentrations are shown by Coomassie blue staining (lanes A and B) and radioactivity levels by autoradiography (lanes C and D). The upper band is [^{14}C]DEPC-treated native R67 DHFR (B, D) and the lower band is [^{14}C]DEPC-treated chymotrypsin-truncated R67 DHFR (A, C). The bottom of the gel is the anode.

DISCUSSION

Dissociation of Tetrameric R67 DHFR into Two Dimers. Our evidence supporting a reversible, two-state dissociation of tetrameric R67 DHFR into two dimers is substantial. First, crystal structures have been obtained for both dimeric and tetrameric R67 DHFR suggesting that, in different solvents, both species are stable [Matthews et al. (1986); Narayana, Matthews, Xuong, personal communication]. Second, a titration in K_{av} from pH 5 to 8 appears in Figure 2 and a 1.8-fold difference in molecular weight at the two pH extremes is observed. Third, ultracentrifugation experiments identify only tetramer at pH 8.01, a mixture of dimer + tetramer at pH 6.50, 6.13, and 5.81, and only dimer at pH 5.01 (Figure 5). Fourth, pH titrations of fluorescence are protein concentration dependent (Figure 3b) and the observed blue shifts for the observed fluorescence are consistent with the bimolecular reaction depicted in Scheme II. Fifth, quenching of tryptophan fluorescence by iodide is substantial at pH 5 and minimal at pH 7.0. Iodide quenches the fluorescence of accessible tryptophan residues, and since iodide is a large anion, only surface tryptophans are quenched. From Figure 1, W38, -138, -238, and -338 occur at the dimer–dimer interface and their solvent accessibility should vary depending on the dimeric or tetrameric state of the protein.

K_d estimates (Table I) range from 9.72 to 262 nM using fluorescence, NMR, and ultracentrifugation techniques. The higher range of calculated K_d values (44–122 nM) from sedimentation equilibrium experiments uses an assumed pK_a of 6.77 from our NMR experiments. If a pK_a of 6.84 (fluorescence experiments) is used, a lower range of K_d values (35.4–93.4 nM) is estimated. If the pK_a is higher still, then the calculated K_d values will decrease even more.

Linkage of Histidine 62 Titration to the T ↔ 2D Equilibrium. Since the association state of R67 DHFR changes between pH 8 to 5, this behavior is probably correlated with ionization of residues that destabilize tetramer. The most sensitive area of the structure affecting tetramer stability should be the dimer–dimer interfaces. From Figure 1, H62 is the most likely candidate for an ionizing residue at the dimer–dimer interface. Schemes I and II propose when H62, -162, -262, and -362 become protonated at low pH, their positive charges become repulsive and force dissociation of tetramer into dimers.

To support the role of histidine in this model, NMR chemical shift data were obtained. Figure 6C depicts a titration of the chemical shift between pH* 5 and 6.62 for the sharp C2 proton peak of H62 in dimeric R67 DHFR. Above pH* 6.62, the sharp C2 proton peak is so small that it cannot be identified. Fitting of the incomplete ionization curve yields a pK_a of ≥6.77.

In a recent report by Rosevear et al. (1992), the chemical shift of the C2 proton of H62 in RBG200 DHFR was determined using [2-^{13}C]His-labeled protein. This enzyme is a synthetic R388 DHFR (a type II DHFR) which is 78%

homologous with R67 DHFR. The nonconserved regions occur at the N- and C-termini. Rosevear et al. found two pK_a values for the H62 C2 proton (6.9, 7.0) which are presumably associated with two different protein conformations.

Since both the T ↔ 2D and His62, -162, -262, and -362 + nH^+ ↔ H_n-His62, -162, -262, and -362 reactions occur and can be studied individually, the question of linkage between these two reactions arises (Wyman & Gill, 1990). Linkage between these two reactions proposes that upon dimer formation at intermediate and low pH values, protonation of H62 occurs, DH_n forms, and tetrameric R67 DHFR is destabilized. Evidence supporting linkage of the H62 ionization with a molecular weight titration includes the observation that chemical modification of H62 by DEPC causes R67 DHFR to elute as a dimer from a molecular sieving column at pH 8.0. Native R67 DHFR elutes as a tetramer at this pH. Additional evidence for linkage is shown in Figure 6D, as NMR peak intensity for the sharp C2 proton of H62 decreases as the pH* increases. Our interpretation of this phenomenon is that changes in sharp peak intensity describe the percent dimer present; i.e., as the concentration of dimeric R67 DHFR decreases, the intensity of the sharp C2 proton peak of H62 decreases. Concurrently, as the concentration of tetramer increases, a new peak at ~7.35 ppm appears and its intensity increases with pH, with a maximum peak intensity at pH 7.0. Finally, and more conclusively, we have recently generated a H62C mutant in R67 DHFR (unpublished data) and find in our preliminary experiments that this protein remains tetrameric between pH 5 and 8 as monitored by molecular sieving techniques. If ionization of H62 is indeed linked to the T ↔ 2D equilibrium, this is exactly the result expected; i.e., upon mutation of H62, there is a concurrent change in the T ↔ 2D equilibrium.

As discussed under Materials and Methods, the reaction T + $2nH^+$ ↔ TH_{2n} ↔ $2DH_n$ (Scheme I) could also theoretically occur in this linked reaction. To determine whether this reaction pathway is significantly populated, we note that the T ↔ 2D reaction can be monitored directly at high pH and the TH_n ↔ $2DH_n$ reaction can be isolated at low pH. The sedimentation equilibrium data indicate the K_d for T ↔ 2D at pH 8 is ≤50 nM and K_e for TH_n ↔ $2DH_n$ at pH 5 is ≥3.8 mM. These results suggest the concentration of TH_n should be insignificantly low and that simplification of Scheme I to Scheme II is reasonable. We note that our experiments are equilibrium studies, however, and to determine the extent of involvement of either pathway would require kinetic experiments.

Our estimates for K_d, K_a, and K_e allow prediction of a value for K_b in Scheme I as $K_a^{2n}/K_d = K_b^n/K_e$. K_e and K_d are dissociation constants, and limits for these values were obtained by sedimentation equilibrium studies at pH 5 and 8, respectively. K_a and K_b are ionization constants, and an estimate of K_a was obtained using NMR. If K_e = 3.8 mM, K_d = 50 nM, and pK_a = 6.77, then pK_b = 8.66 (n = 1) or pK_b = 11.1 (n = 2). These values are both significantly higher than the estimated pK_a values, suggesting ionization of H62 is significantly affected by its environment.

The number of protons added per dimer could be either one or two assuming that only H62 ionization is involved in Scheme II. Addition of only one proton per dimer would occur if a hydrogen bond existed between H62 and H362 (and H162 and H262) at the dimer–dimer interfaces. This would be analogous to the interaction in pepsin where a hydrogen bond between protonated Asp215 and ionized Asp32 exists and results in altered pK_a values [4.5 and 1.1, respectively; Cornish-Bowden and Knowles (1969) and James and Sielecki (1983)]. Alternatively, if such a hydrogen bond does not exist at the dimer–dimer interfaces in R67 DHFR, two protons per dimer can be added. Best fits to the K_{av} and sedimentation equilibrium data yield n = 1; however, best fits to the fluorescence and NMR intensity data indicate n = 2. [Note, fitting of the NMR chemical shift data indicates n = 1; however, according to Markley (1975), this value measures cooperativity between titrations.] The discrepancy between the values for n from these various fits indicates that either n cannot be accurately determined with these methods or the underlying assumptions employed to interpret the data from the various techniques are only approximations. However, as argued above, this discrepancy does not invalidate our overall model and estimates of pK_a and K_d.

To ascertain the value of n more clearly, it would be helpful to have a fully refined tetrameric crystal structure. The distance between H62 and H362 could then be measured to determine whether a hydrogen bond is implied. In addition, NMR spectra with ^{13}C-labeled histidine might allow generation of a complete titration curve and the number of protons associated with tetrameric R67 DHFR counted directly.

Dimeric R67 DHFR Activity. While our data are limited at present, they are consistent with a model where tetrameric R67 DHFR is active and dimeric R67 DHFR is inactive or only partially active. Modification of H62 by DEPC stabilizes dimeric DHFR and yields a protein with decreased k_{cat} and increased K_m values. The overall decrease in k_{cat}/K_m is 200–600-fold. Since modification using [^{14}C]DEPC indicates incomplete modification (2.7 histidines/tetramer), the observed catalytic efficiencies may be higher than for a totally modified enzyme. We note K_m values for R67 DHFR modified by DEPC are 7–24-fold higher than unmodified values, suggesting that the activity observed was not totally due to contaminating or hydrolyzed unmodified R67 DHFR.

Decreased activity associated with dimeric R67 DHFR would also help explain pH profiles obtained by Morrison and Sneddon (1990) and Brito et al. (1990). These pH profiles show decreased activity at pH ≤5.4–6, where R67 DHFR is predominantly dimeric.

An alternate conclusion from the DEPC modification studies would suggest that the modification of H62, not the consequent dissociation of tetramer, causes loss of enzyme activity. This interpretation seems less probable as Figure 1 indicates H62 occurs at the dimer–dimer interface, not in the putative active site pore. Also, preliminary kinetic analysis of our mutant H62C R67 DHFR indicates this DHFR is still quite active.

Any in vivo significance of the T ↔ 2D + $2nH^+$ ↔ $2DH_n$ equilibria is unclear. It may be a method of controlling enzyme activity as a function of pH and protein concentration. Alternatively, these linked equilibria may have been important in the original function of type II DHFRs. Since type II DHFRs were recruited by bacteria to provide TMP resistance and to catalyze the reduction of DHF (albeit inefficiently), the original function of this gene sequence is unknown. Stone and Smith (1979) have hypothesized that type II DHFRs were originally general NADP-linked oxidoreductases that were recruited to catalyze the DHFR reaction. To our knowledge, this hypothesis has not been tested and the original function of type II DHFR genes has not been identified yet.

ACKNOWLEDGMENT

We thank Dave Matthews, Narendra Narayana, and Nguyen-huu Xuong for sharing their crystal structure data; Michael Johnson for a copy of NONLIN; Allan P. Minton

for help with the hardware and software interface for the ultracentrifuge; Engin Serpersu and Jay Gregory for initial NMR scans and discussions; and Charles Linn for his excellent technical assistance.

REFERENCES

Amyes, S. G. B. (1989) *J. Med. Microbiol. 28*, 73–83.

Amyes, S. G. B., & Smith, J. T. (1974) *Biochem. Biophys. Res. Commun. 58*, 412–418.

Amyes, S. G. B., Towner, K. J., Carter, G. I., Thomson, C. J., & Young, H. K. (1989) *J. Antimicrob. Chemother. 24*, 111–119.

Amyes, S. G. B., Towner, K. J., & Young, H. K. (1992) *J. Med. Microbiol. 36*, 1–3.

Baccanari, D., Phillips, A., Smithe, S., Sinski, D., & Burchall, J. (1975) *Biochemistry 14*, 5267–5273.

Blakley, R. L. (1960) *Nature 40*, 1684–1685.

Brisson, N., & Hohn, T. (1984) *Gene 28*, 271–275.

Brito, R. M. M., Reddick, R., Bennett, G. N., Rudolph, F. B., & Rosevear, P. R. (1990) *Biochemistry 29*, 9825–9831.

Cornish-Bowden, A. J., & Knowles, J. R. (1969) *Biochem. J. 113*, 353–362.

Doyle, M. L., Speros, P. C., LiCata, V. J., Gingrich, D., Hoffman, B. M., & Ackers, G. K. (1991) *Biochemistry 30*, 7263–7271.

Eftink, M. R., & Ghiron, C. A. (1981) *Anal. Biochem. 114*, 199–227.

Ellis, K. J., & Morrison, J. F. (1982) *Methods Enzymol. 87*, 405–426.

Flensburg, F., & Steen, R. (1986) *Nucleic Acids Res. 14*, 5933.

Fling, M. E., Kopf, J., & Richards, C. (1988) *Plasmid 19*, 30–38.

Gornall, A. G., Bardawill, C. J., & David, M. M. (1949) *J. Biol. Chem. 177*, 751–766.

Holbrook, J. J., & Ingram, V. A. (1973) *Biochem. J. 131*, 729–738.

Horecker, B. L., & Kornberg, A. (1948) *J. Biol. Chem. 175*, 385–390.

Huovin, P. (1987) *Antimicrob. Agents Chemother. 31*, 1451–1456.

James, M. N. G., & Sielecki, A. R. (1983) *J. Mol. Biol. 163*, 299–361.

Jansson, C., & Skold, O. (1991) *Antimicrobiol. Agents Chemother. 35*, 1891–1899.

Johnson, M. L., & Fraser, S. G. (1985) *Methods Enzymol. 117*, 301–342.

Johnson, M. L., Halvorson, H. R., & Ackers, G. K. (1976) *Biochemistry 15*, 5363–5371.

Joyner, S. S., Fling, M. E., Stone, D., & Baccanari, D. P. (1984) *J. Biol. Chem. 259*, 5851–5856.

Kraut, J., & Matthews, D. A. (1987) *Biological Macromolecules and Assemblies* (Jurnak, F. A., & Mcpherson, A., Eds.) Vol. 3, pp 1–71, Wiley, New York.

Kurzban, G. P., Gitlin, G., Bayer, E. A., Wilchek, M., & Horowitz, P. M. (1989) *Biochemistry 28*, 8537–8542.

Lakowitz, J. R. (1983) *Principles of Fluorescence Spectroscopy*, Plenum Press, New York.

Loewenthal, R., Sancho, J., & Fersht, A. R. (1991) *Biochemistry 30*, 6775–6779.

Lundblad, R. L., & Noyes, C. M. (1984) *Chemical Reagents for Protein Modifications*, Vol. 1, CRC Press, Boca Raton, FL.

Markley, J. L. (1975) *Acc. Chem. Res. 8*, 70–80.

Matthews, D. A., Smith, S. L., Baccanari, D. P., Burchall, J. J., Oatley, S. J., & Kraut, J. (1986) *Biochemistry 25*, 4194–4204.

Miles, E. W. (1977) *Methods Enzymol. 47*, 431–422.

Morrison, J. F., & Sneddon, M. K. (1990) in *Chemistry and Biology of Pteridines 1989* (Curtius, H.-Ch., Ghisla, S., & Blau, N., Eds.) pp 728–733, Walter de Gruyter, Berlin.

Parsons, Y., Hall, R. M., & Stokes, H. W. (1992) *Antimicrob. Agents Chemother. 35*, 2436–2439.

Pattishall, K. H., Acar, J., Burchall, J. J., Goldstein, F. W., & Harvey, R. J. (1977) *J. Biol. Chem. 252*, 2319–2323.

Poe, M. (1973) *J. Biol. Chem. 248*, 7025–7032.

Potschka, M. (1987) *Anal. Biochem. 162*, 47–64.

Reece, L. J., Nichols, R., Ogden, R. C., & Howell, E. E. (1991) *Biochemistry 30*, 10895–10904.

Roarke, D. E. (1976) *Biophys. Chem. 5*, 185–196.

Rosevear, P. R., Krudy, G. A., Brito, R. M. M., Williams, J. S., & Rudolph, F. B. (1992) *FASEB J. 6*, A417.

Salter, D. N., Ford, J. E., Scott, K. J., & Andrews, P. (1972) *FEBS Lett. 20*, 302–306.

Skold, O., & Widh, A. (1974) *J. Biol. Chem. 249*, 4324–4325.

Smith, G. M., & Mildvan, A. S. (1981) *Biochemistry 20*, 4340–4346.

Smith, S., & Burchall, J. J. (1983) *Proc. Natl. Acad. Sci. U.S.A. 80*, 4619–4623.

Smith, S., Stone, D., Novak, P., Baccanari, D. P., & Burchall, J. J. (1979) *J. Biol. Chem. 254*, 6222–6225.

Stone, D., & Smith, S. (1979) *J. Biol. Chem. 254*, 10857–10861.

Sundstrom, L., Vinayagamoorthy, T., & Skold, O. (1987) *Antimicrob. Agents Chemother. 31*, 60–66.

Sundstrom, L., Radstrom, P., Swedberg, G., & Skold, O. (1988) *MGG, Mol. Gen. Genet. 213*, 191–201.

Swift, G., McCarthy, B. J., & Heffron, F. (1981) *MGG, Mol. Gen. Genet. 181*, 441–447.

Vermersch, P. S., Klass, M. R., & Bennett, G. N. (1986) *Gene 41*, 289–297.

Wylie, B. A., & Koornhof, H. J. (1991) *J. Med. Microbiol. 35*, 214–218.

Wylie, B. A., Amyes, S. G. B., Young, H. K., & Koornhof, H. J. (1988) *J. Antimicrob. Chemother. 22*, 429–435.

Wyman, J. (1964) *Adv. Protein Chem. 19*, 223–286.

Wyman, J., & Gill, S. J. (1990) *Binding and Linkage*, University Science Books, Mill Valley, CA.